4
Black Chrome-Graphite Encapsulated FeCo NPs Composite Solar Selective Coatings

4.1 INTRODUCTION

Black chrome ($Cr\text{-}Cr_2O_3$) is one of the extensively studied and a commercialized spectrally selective absorber coating for photothermal applications. Historical development of black chrome (BC) spectrally selective absorbers has already been reviewed in sections 2.4.2. Several deposition techniques are used to deposit this spectrally selective absorber coating, explained briefly in sections 2.3. Among them, electrodeposition is one of the widely used deposition technique due to its simplicity, low cost, and scalability towards large and curved surfaces [Quintana and Sebastian, 1994]. This deposition process is also suitable for the development of coatings with high solar absorptance, good stability in a wide range of oxidizing/reducing environments and high thermal resistance [Hamid, 2009]. Several studies are reported on the development of the electrodeposited black chrome coatings on numerous substrates like stainless steel (SS), copper (Cu), and bright nickel coated Cu etc. Some of such black chrome spectrally selective coatings have been commercialized for solar thermal applications [Eugénio *et al*., 2011; Bogaerts and Lampert, 1983; Duffie and Beckman, 1980; Schlesinger and Paunovic, 2000; Endres, *et al.,* 2008; Endres, 2002; Zein El Abedin *et al*., 2004; Endres *et al*., 2003; Mukhopadhyay *et al*., 2005; Ali *et al*., 1997].

The thickness of these coatings is very important and has an impact on solar thermal properties, especially the environmental impacts such as corrosion and related degradation. For example, the low thickness of such coatings cannot protect the substrate against atmospheric corrosion and thermal oxidation. A bright nickel coating, prior to the black chrome deposition, was recommended to solve the substrate corrosion problem to a small extent [Daryabegy and Mahmoodpor, 2006]. The electrochemical characterization of black chrome coatings, corrosion analysis of black chrome coatings, thermal behavior and the associated decomposition mechanisms and pathways have been studied in detail by several research groups across the globe [Abbott *et al*., 2004; Ithurbide *et al*., 2007; Al-Kuhaili and Durrani, 2007; Perissi *et al*., 2006; Danilov *et al*., 2001; Song and Chin, 2002; Lampert and Washburn, 1979; Sweet *et al*., 1984; Inal *et al*., 1981; Mabon *et al*., 1982; Driver and McCormick, 1982; Surviliene *et al*., 1999; Zajac *et al*., 1980]. In order to understand the effect of corrosion on the optical properties of black chrome coatings, especially absorptivity (α) and emissivity (ε) were measured before and after corrosion tests in marine environment [Dibari and Turillon, 1979]. The thermal degradation of black chrome and the correlation of oxide content in black chrome coatings and their optical properties have been intensively studied and reported extensively in the literature [Grimmer and Collier, 1981; Hogg and Smith, 1977; Holloway *et al*., 1980; Ignatiev *et al*., 1979a; Ignatiev *et al*., 1979b]. In conjunction with optical properties, other physical properties, such as mechanical properties, thermal stability (in air and vacuum), corrosion analysis and its effects on solar thermal properties of electrodeposited black chrome coatings are studied and reported in the literature [Murr *et al*., 1980; Prasad *et al*., 1980; Rajagopalan *et al*.,1978; Reiss, 1981; Ritchie *et al*., 1979; Spitz *et al*., 1979; Valayapetre *et al*., 1979; Window *et al*., 1979; Zajac and Ignatiev, 1979; McDonald, 1975; Jafari and Rozati, 2011]. Nevertheless, studies on improving the corrosion and thermal stability of black chrome coatings are always attracting attention for enhanced solar thermal performance in ambient conditions. We have attempted the same introducing

nanoparticle in the black chrome selective coatings, which has not been explored much. Therefore, an attempt has been made to enhance the thermal stability using high temperature and environmentally stable graphite encapsulated FeCo nanoparticles (FeCo(C) NPs), into black chrome coatings for their application at or above 250 ^{o}C temperature.

4.2 BLACK CHROME-GRAPHITE ENCAPSULATED FeCo NPs COMPOSITE SPECTRALLY SELECTIVE COATINGS

The thermal stability of black chrome spectrally selective coatings is still a challenge for their application at or above 250 ^{o}C. This is mainly due to the oxidation of metallic chromium in black chrome coatings at elevated temperature. The diffusion of environmental oxygen is responsible for such degradation, where oxygen reacts chemically with metallic chromium, converting into chromium oxide. Thus, it is important to protect the oxidation of metallic content for its application at higher temperatures. Graphite encapsulated FeCo nanoparticles (FeCo(C) NPs) is of particular interest because of their high temperature and chemical/environmental stability and that's why selected for the present study [Seo *et al.*, 2006; Turgut *et al.*, 1998; Desvaux *et al.*, 2005; Lee *et al.*, 2011; Poddar *et al.*, 2004; Chu *et al.*, 1999; Xu *et al.*, 2013]. The average particles size of FeCo(C) NPs, used in this work, is in the range ~ 30 to 35 nm, with ~ 25 nm diameter of FeCo alloy as core and ~ 10 nm thick onion type lattice fringes of graphite carbon as shell [Gupta *et al.*, 2014]. These nanoparticles can be used to protect the metallic chromium nanostructures and thus may avoid the thermal oxidation of metallic chromium under ambient and elevated temperature conditions. A schematic representation of FeCo(C) NPs encapsulated metallic chromium content is shown in Figure 4.1. The upper part of the schematic, Figure 4.1, represents the metal chromium particles inside the chromium oxide (Cr_2O_3) matrix, forming a black chrome solar selective film, on a copper substrate. The lower part of the schematic, Figure 4.1, explains the formation of FeCo(C) nanoparticles protecting layer around the metallic chromium, inside the chromium oxide matrix, in nanoparticles modified black chrome spectrally selective coatings on a copper substrate. The middle portion of Figure 4.1 represents zoomed region of FeCo(C) NPs covered Cr nanostructured metallic components. Thus, the high temperature and environment/chemical stability of FeCo(C) NPs may protect the oxidation of chromium metallic content. This may be the region of observed higher thermal and corrosion stabilities of such FeCo(C) NPs modified black chrome spectrally selective coatings.

4.3 EXPERIMENTAL PROCEDURE

0.5 mm thick Copper (Cu) and stainless-steel (SS) sheets were cut into 2.5 cm x 1 cm pieces and used as substrates for black chrome electrodeposition. All these substrates were mechanically polished with (number: 120) sand paper, followed by rinsing in distilled water. After polishing, substrates were degreased for ~ 10 min with trichloroethylene and acetone, followed by distilled water rinsing and finally dried in air at room temperature. An infrared reflector layer of Ni has been deposited using a two electrode electrochemical cell, where Copper (Cu), Ni/Cu (Ni-coated copper) and stainless-steel (SS) substrates are used as cathode and PbSb alloy, with 2 – 5% Sb, is used as an anode. The electrolytic bath for Ni-coating consists of nickel sulfate; 250g/l, nickel chloride; 60g/l, boric acid: 40g/l and pH of the solution has been maintained at 3.5 during the deposition process. The electrolytic bath was homogenized using magnetic stirrer at 200rpm before initiating the electrochemical process under galvanostatic conditions. The current densities are varied from 0.2 A/cm^2 to 0.30 A/cm^2 and the time of deposition has also been varied from the 60s to 120s to optimize the nickel layer on the copper substrate. The deposited Ni/Cu and Ni/SS samples were rinsed with deionized water to remove any residual debris and dried using hot air. The electrolytic bath for black chrome (BC) spectrally selective coating is composed of CrO_3: 275g/l, NaF: 0.2g/l and $NaNO_3$: 3g/l in water-based media. The electrolytic bath for FeCo(C) NPs modified black chrome spectrally selective

coatings has been modified using 0.025, 0.05, and 0.10 wt.% of FeCo(C) NPs in BC electrolyte solution. The pH of the electrolytic bath has been maintained at 0.3 during all the deposition experiments.

BC and FeCo(C) NPs modified BC spectrally selective coatings are deposited using the two electrodes electrochemical cell as used for Ni layer deposition, at current densities ranging from 0.60 A/cm² to 0.80 A/cm² for 3600s. The deposited BC/Cu; BC/Ni/Cu; BC/SS; BC-FeCo(C)/Cu; BC- FeCo(C)/Ni/Cu and BC-FeCo(C)/SS samples were rinsed with deionized water to remove any residual debris and dried using hot air.

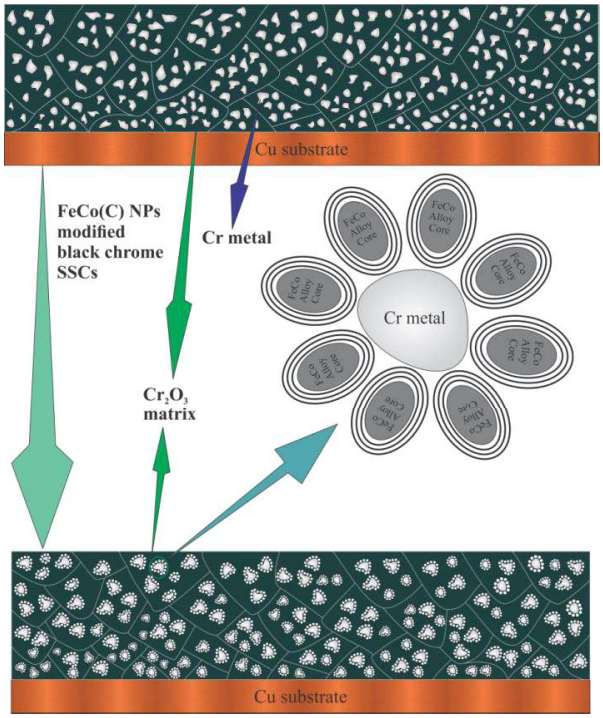

Figure 4.1 : Schematic representation of black chrome and FeCo(C) NPs modified black chrome composite spectrally selective absorbers on Cu substrate.

We carried out X-ray diffraction (XRD) measurements to understand the development of phases and structures for the deposited thin film cermet (metal-dielectric composite) coatings. XRD graphs were recorded in the range of 20° to 80° with 0.02° step size using copper K_α radiation (λ= 1.5406Å). The microstructural and surface properties, such as roughness and grain size, were investigated using scanning electron microscope (SEM) and atomic force microscope (AFM) measurement systems. All AFM micrographs were recorded on 20 x 20 μm² and 10 x 10 μm² scanning areas, with 256 x 256 pixel resolutions. The samples were scanned in contact mode (CONTSCR cantilever tip with a radius of curvature < 10 nm) under ambient conditions. Elemental compositions were calculated using energy dispersive X-ray (EDX) measurement system, equipped as an accessory with SEM equipment. Cary 4000 UV-Vis spectrophotometer was used to calculate absorptance of the selective absorber and FTIR spectrophotometer was used to calculate the emittance values for the synthesized spectrally selective coatings. Electrochemical studies on these coatings were done in 3.5 wt.% NaCl (saline) solution employing Iviumstat spectro-electrochemical workstation to understand the corrosion properties of these coating structures. BC and BC-FeCo(C) NPs composite selective coatings deposited on Cu, Ni/Cu, and SS substrates act as the working electrode, Ag/AgCl, and

platinum as reference and counter electrode for the corrosion and cyclic voltammetry studies. Tafel analysis has been used to calculate the corrosion current density, corrosion resistance and corrosion rates. Thermal analyses of these coatings were carried out using Perkin – Elmer Simultaneous Thermal Analyzer (STA) up to 900^0C temperatures under N_2 atmosphere, at 10 °C min^{-1} heating rate on pristine and corrosion treated coating structures. These studies assisted in understanding the microstructural changes and their impact on solar thermal properties for developed spectrally selective coating structures.

4.4 RESULTS AND DISCUSSION

4.4.1 X-ray Diffraction Analysis

X-ray diffraction spectra are shown in Figure 4.2 (left panel) a(i) and a(ii, iii & iv) for pristine and FeCo(C) NPs modified black chrome composite spectrally selective coatings, deposited on copper substrates. Pristine black chrome (BC) selective coatings exhibit only hexagonal phase of chromium (Cr) at 2θ = 38.40°, 43.72° and 69.25°; corresponding to (100), (101) and (110) diffraction peaks (ICDD PDF #: 01-074-7045) (Fig. 4.2 a(i)). However, with modifying FeCo(C) NPs, it also consist a (110) diffraction peak at 2θ = 44.40° of iron cobalt alloy phase (FeCo) (ICDD PDF #: 65-6829) (Fig. 4.2 a(ii, iii, iv)) [Gupta *et al.*, 2014]. This suggests the presence of NPs, which modified the pristine black chrome selective coatings. Moreover, there are no diffraction peaks for chromium oxide (Cr_2O_3) crystallographic phase, suggesting that the chromium oxide is present in amorphous form in these selective absorber coatings.

Figure 4.2 (right panel) shows the X-ray diffraction spectra of black chrome (Fig. 4.2 b(i)) and modified black chrome (Fig. 4.2 b(ii, iii, iv)) selective coatings on nickel coated copper substrates. These XRD patterns also confirm the hexagonal chromium phase in pristine black chrome (Fig. 4.2 b(i)) and (110), (200) iron cobalt (FeCo) phase at 2θ = 44.40°, 64.62° with hexagonal chromium phase in modified black chrome selective coatings (Fig. 4.2 b(ii, iii, iv)). The black chrome and modified black chrome coatings on SS substrate also show identical crystallographic phases like Cu and Ni/Cu substrates. The increased concentration of FeCo(C) nanoparticles in black chrome electrolyte resulted into the enhanced FeCo(C) concentration in black chrome thin films. This enhancement has been clearly observed in XRD graphs, where (110) plane FeCo alloy peaks became intense with increasing FeCo(C) concentration. In spite of large fraction FeCo(C) nanoparticles, metallic chromium diffraction peak can be observed, suggesting that FeCo(C) NPs covering may be very thin on metallic chromium, as indicated schematically in Figure 4.1.

4.4.2 Microstructural Analysis

Scanning electron micrographs are shown in Figure 4.3 (a, b, c & d), for black chrome and FeCo(C) NPs modified black chrome selective coatings. The black chrome coatings surface micrographs are smooth with micron size grains, exhibiting large cracks, as can be seen in Figure 4.3a. The films became coarser with respect to pristine black chrome coatings after increasing FeCo(C) NPs concentration in modified black chrome coatings. However, with enhanced coarseness, the films have shown enhanced uniformity with lesser cracks, and smaller grains. The thicknesses of these coatings are kept at higher side, ~ 10 μm, intentionally, as these films have been subjected to the thermal stresses and corrosion environments to understand their degradation and associated structure-property relation.

Figure 4.4 shows the SEM micrographs of back chrome (a) and FeCo(C) NPs modified black chrome selective coatings (b, c & d) on nickel coated copper substrates. The surface micrographs of black chrome selective coatings suggest micron size grains, similar to that of black chrome coatings on the copper substrates only. Here also, cracks (Fig. 4.4a) are visible throughout the film. The FeCo(C) NPs modified black chrome selective coatings show the

coarser structure with less prominent cracks, as can be seen in Fig. 4 (b, c & d). The thicknesses of these coatings are ~ 12 µm, as shown in the cross-section SEM image for one of the structure, Figure 4.4 e.

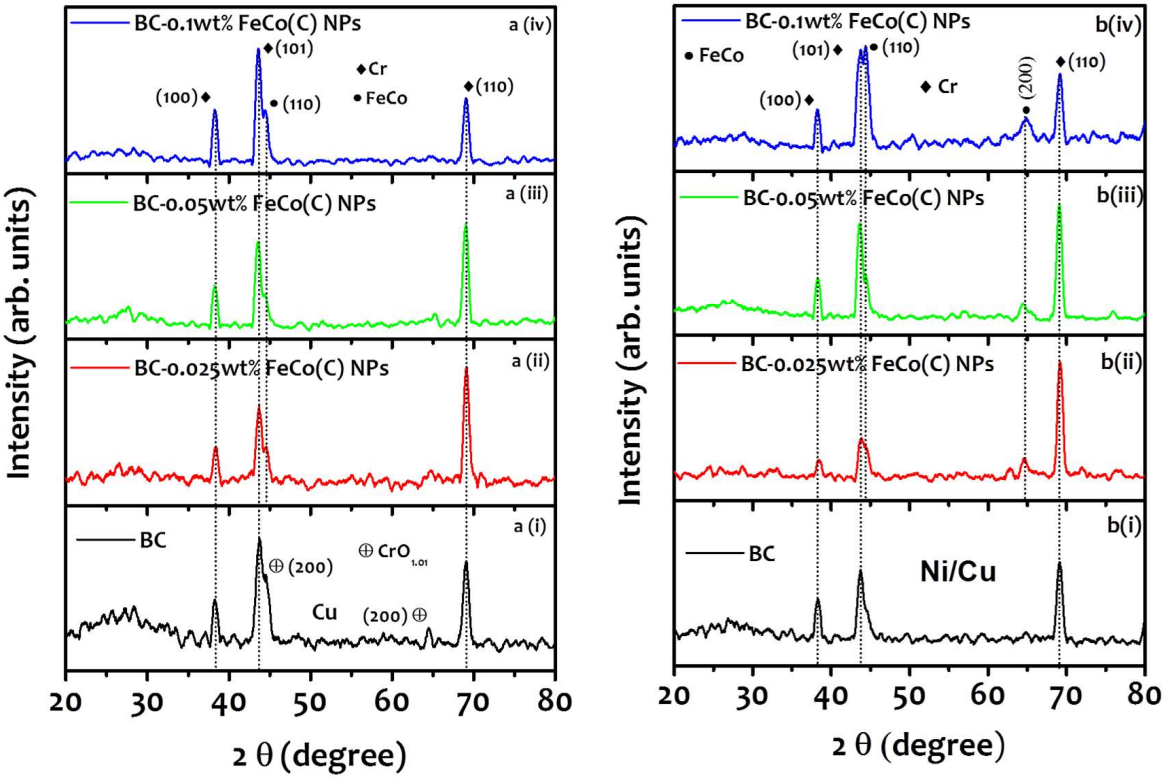

Figure 4.2 : X-ray diffraction spectra of (a&b)(i) black chrome and (a&b)(ii, iii, iv) FeCo(C) NPs modified black chrome selective coatings with varying wt.% of FeCo(C) NPs deposited on (left panel) copper (Cu) and (right panel) nickel coated (Ni/Cu) substrates.

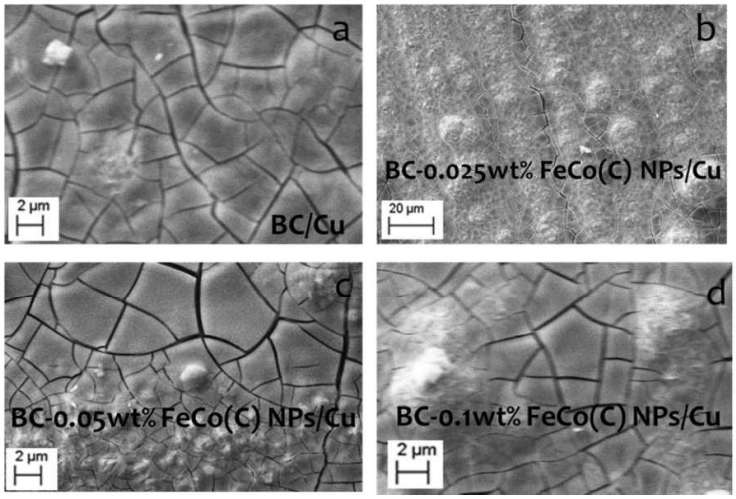

Figure 4.3 : (a) SEM micrographs of black chrome and (b, c & d) FeCo(C) NPs modified black chrome with varying wt% of FeCo(C) NPs selective surfaces deposited on copper substrates.

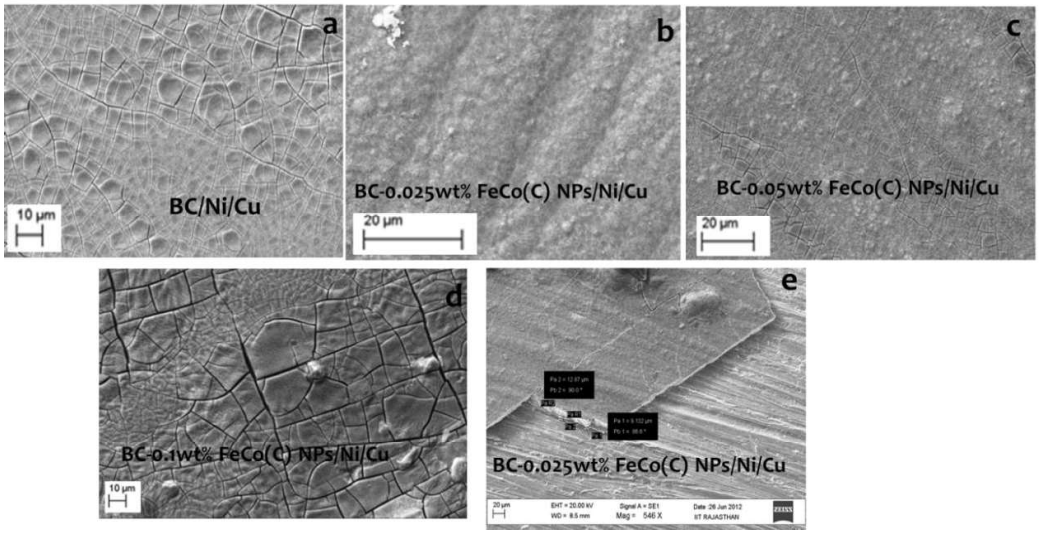

Figure 4.4 : (a) SEM micrographs of black chrome and (b, c&d) FeCo(C) NPs modified black chrome with varying wt.% of FeCo(C) NPs selective surfaces deposited on copper substrate. (d) SEM cross-section of thickness measurements.

In continuation, to further understand the microscopic structural details, AFM surface measurements are carried out for black chrome and FeCo(C) NPs modified black chrome selective coatings deposited on nickel coated copper substrate. These AFM images are shown in Figure 4.5 (a, b, c & d). Black chrome selective coatings show striped wrinkles like surface morphology (Fig. 4.5a), whereas, island type surface morphology has been observed for FeCo(C) NPs modified black chrome selective coatings, Figure 4.5b. In addition, FeCo(C) NPs modified black chrome selective coatings exhibit less average surface roughness (R_a) as compared to the pristine black chrome selective coatings (Fig.4.5, right panel), consistent with SEM observations, as discussed earlier.

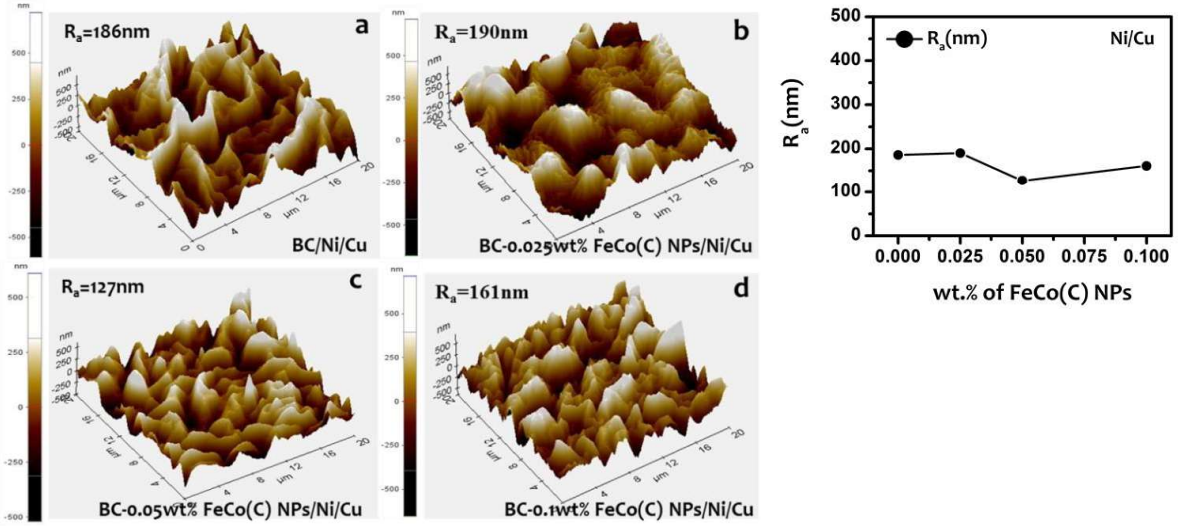

Figure 4.5 : (right panel) AFM surface morphology (a) of black chrome and (b, c&d) FeCo(C) NPs modified black chrome with varying wt.% of FeCo(C) NPs selective surfaces deposited on nickel coated copper substrate. (Left panel) Average roughness vs. wt.% of FeCo(C) NPs.

4.4.3 Elemental Analysis

The elemental results are summarized in Fig. 4.6 (a, b, c & d) for black chrome and different wt.% of FeCo(C) NPs modified black chrome selective coatings on copper substrates. These energy-dispersive X-ray spectra of black chrome selective coating show the chromium (Cr) and oxygen (O) elemental peaks only (Fig. 4.6a). The corresponding elemental compositions are listed in the insets of respective spectra in both weight% and atomic% (Fig.4.6a). The observed elemental fraction of oxygen and chromium are 74.58 atm.%, and 25.42 atm.% respectively, suggesting the presence of chromium oxide phase in these coatings. The FeCo(C) NPs modified black chrome selective coatings show additional Fe elemental peak with Cr and O peaks, similar to that of pristine black chrome coating (Fig.4.6 b, c & d). The 0.025 wt.% FeCo(C) NPs modified black chrome coatings have shown very poor Fe, Co and C elemental fraction ~ 0.05 atm.%, 0.06 atm.% and 8.04 atm.% respectively, (Fig.4.6 b). This may be due to the small fraction of FeCo(C) in the coatings. Moreover, with increasing weight percent of FeCo(C) NPs, iron content has increased, as can be seen in Figure 4.6 (c & d). These measurements were carried out at different sections across the surfaces for different coatings and observed that even with the least wt.% FeCo(C) NPs modified black chrome spectrally selective coatings, Fe, Co and C elemental compositions are distributed uniformly, suggesting homogeneous distribution of FeCo(C) nanoparticles within the coating structures. Elemental composition of black chrome and FeCo(C) NPs modified black chrome selective coatings on nickel coated copper substrates have also shown identical elemental distribution and results are discussed by Usmani et al. in their published work [Usmani and Harinipriya, 2013].

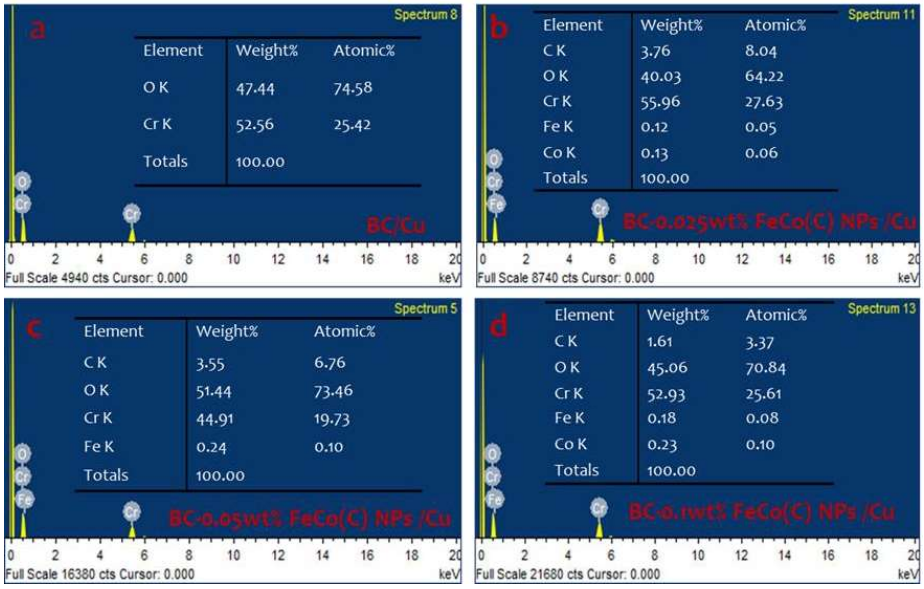

Figure 4.6 : EDS elemental analysis of (a) black chrome and (b, c&d) FeCo(C) NPs modified black chrome with varying wt.% of FeCo(C) NPs selective surfaces deposited on the copper substrate.

4.4.4 Optical Properties

UV-Vis reflectance spectra were collected in 200 – 800 nm wavelength range and are plotted in Figure 4.7 (a & b) for both black chrome and FeCo(C) NPs modified black chrome selective coatings on copper and nickel coated copper substrates. These reflectance data are used to calculate the absorptance values and are summarized in the insets of respective reflectance plots against the weight percent of FeCo(C) NPs coating, Figure 4.7 (a & b) insets, on both Cu and nickel coated Cu substrates. Absorptance values are 0.952, 0.928, 0.933 and 0.941 of

BC and FeCo(C) NPs modified BC on Cu substrates and are 0.946, 0.945, 0.935 and 0.945 of BC and FeCo(C) NPs modified BC on nickel coated copper substrates. These absorptance values are relatively insensitive to FeCo(C) modifications, suggesting that the addition of FeCo(C) metallic nanoparticles has no significant contribution to the absorption as these values are close to the pristine black chrome structures. The observed broad minima at ~ 250 nm and at ~ 350 nm, correspond to intraband 3d transitions in Cr metal and FeCo alloys and are consistent with reported literature [Quinten, 2011]. These minima suggests that along with Cr, FeCo nanoparticles may also be contributing to the strong absorption > ~ 0.95 in the solar spectrum region.

The emittance values of these coating structures are calculated using infrared reflectance and are plotted in Figure 4.8, for BC and FeCo(C) NPs modified BC in 2.5 – 25 μm wavelength range. The calculated emittance values are presented in the inset of Figure 4.8. These emittance values of black chrome and FeCo(C) NPs modified black chrome selective coatings are relatively higher and show variation from 0.47 to 0.66. The large thickness ~10 μm of these structures is the main reason for such high emittance values. It can be decreased up to 0.1 or close to the literature values for black chrome structure by reducing the thickness and optimizing the metallic content. However, the optical properties are not the main objective for this work and that's why thicknesses of these coatings were kept large intentionally, to understand the thermal stability of these coatings through thermogravimetric analysis and the microscopic origin of degradation using different structure-property correlations.

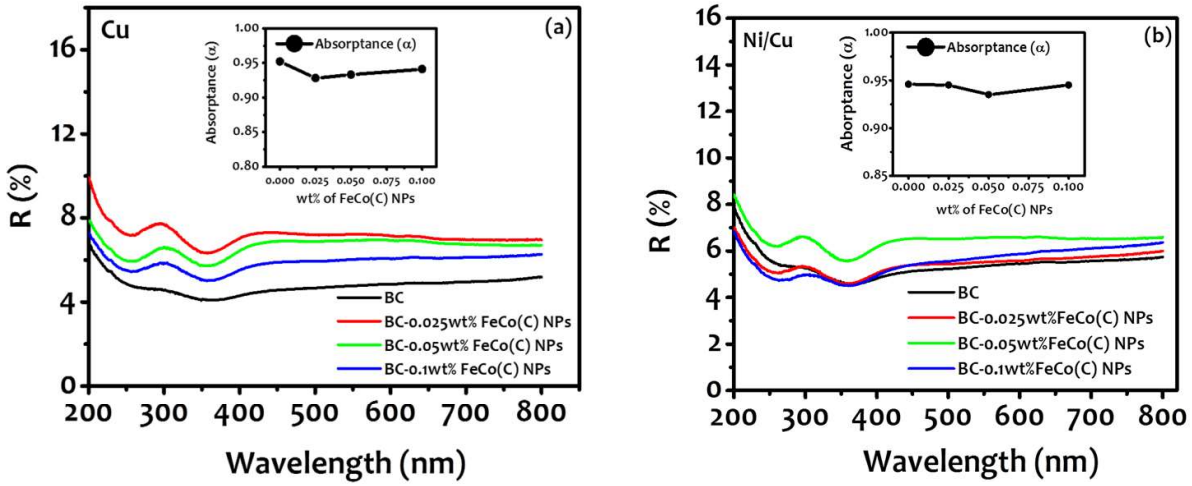

Figure 4.7 : reflectance spectra versus wavelength of black chrome and FeCo(C) NPs modified black chrome with varying wt.% of FeCo(C) NPs selective coatings deposited on (a) Cu and (b) nickel coated Cu substrates. Calculated absorptance values vs. varying wt.% of FeCo(C) NPs are represented an inset in the graphs a & b.

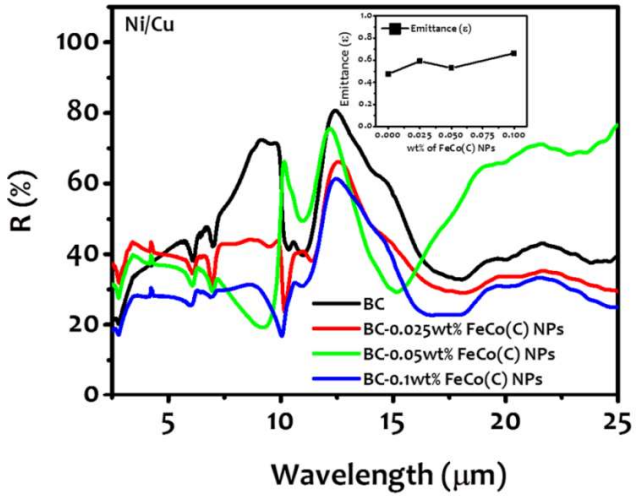

Figure 4.8 : reflectance spectra versus wavelength in the range of 2.5 – 25 μm of black chrome and FeCo(C) NPs modified black chrome with varying wt.% of FeCo(C) NPs selective coatings deposited on nickel coated Cu substrates. Calculated emittance values vs. varying wt.% of FeCo(C) NPs have represented an inset in the graphs.

4.4.5 Electrochemical Measurements

Environmental degradation, especially due to the humidity, salinity, and temperature etc., may hamper the response of black chrome spectrally selective coatings. Thus, it is important to understand the degradation mechanism, which may assist in developing environmentally stable coating structures. Corrosion studies have been carried out using linear voltammetry measurements and the related analysis is discussed below.

4.4.5.1 Cyclic Voltammetry

The electrochemical studies, such as cyclic voltammetry (CV), were carried out in 3.5 wt.% NaCl saline solution to understand the redox process and its effect on the selective coatings. The cyclic voltammograms are shown in Figure 4.10, for black chrome and different wt.% FeCo(C) NPs modified black chrome coatings on the copper substrate. These measurements are recorded at different scan rates (from 5 to 200 mVs^{-1}), in 3.5 wt.% NaCl (saline) solution.

These voltammograms Fig. 4.9 (i, ii, iii & iv), suggest that the current gap between anodic and cathodic scan increases with increasing scan rates. This could be attributed to the change in the diffusion rates of ions or mass transfer from the bulk of the solution to the electric double layer (the interface between an electrolyte solution and an electrode). A schematic model of electrode-solution interface (double layer) is illustrated in Figure 4.10. This explains the contribution of bulk solution in the formation of inner and outer Helmholtz plane, the diffusion layer in contact with electrode during cyclic voltammetry measurements. More surprisingly, these cyclic voltammetry measurements do no exhibit specific redox peaks corresponding to any electrochemical oxidation/reduction process, indicating that the coatings are electrochemically stable even in highly saline environmental conditions.

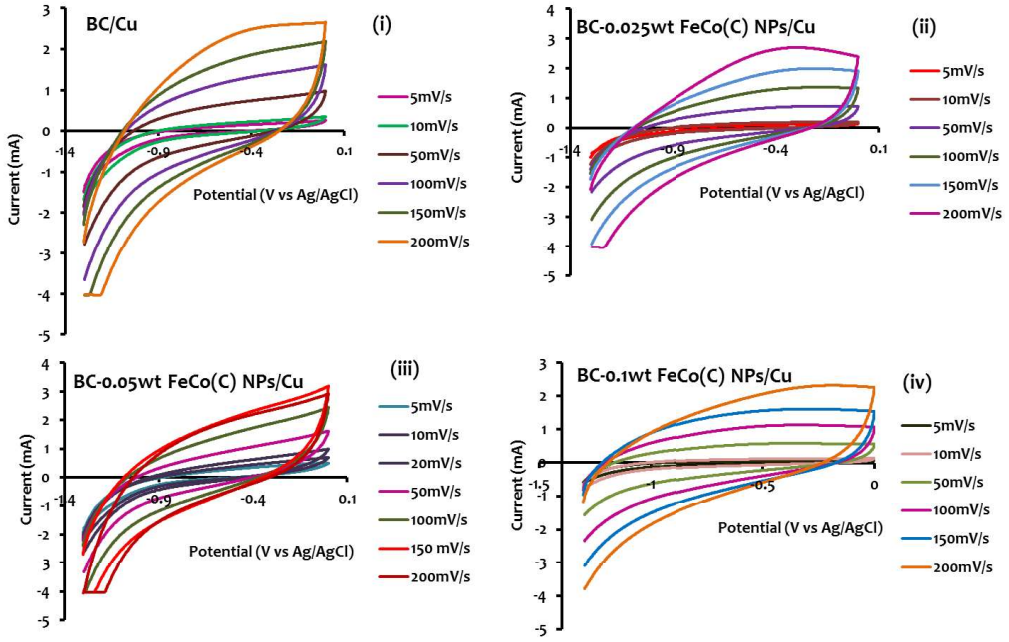

Figure 4.9 : Cyclic voltammogram of **(i)** black chrome and **(ii, iii & iV)** FeCo (C) NPs modified black chrome selective coatings with varying wt.% of FeCo(C) NPs deposited on copper substrate, recorded with different scan rate (from 5 to 200 mVs-1), in 3.5 wt.% NaCl (saline) solution.

Figure 4.11 shows the cyclic voltammograms of black chrome and FeCo(C) NPs modified black chrome with varying wt.% of FeCo(C) NPs selective coatings on nickel coated copper substrate, recorded at different scan rate (from 5 to 200 mVs^{-1}). These voltammograms also do not exhibit any specific redox peak corresponding to any electrochemical oxidation or reduction, suggesting that these coatings are also electrochemically stable in the highly saline environment.

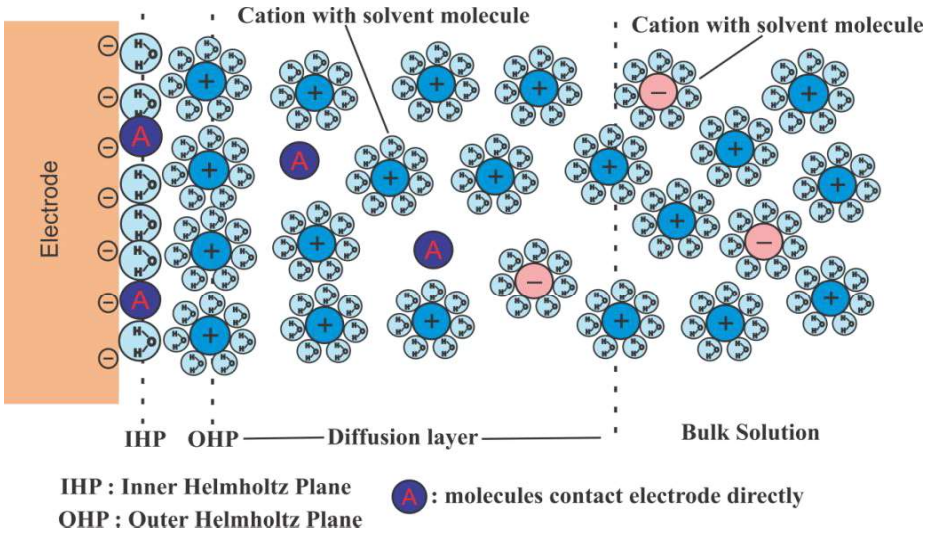

Figure 4.10 : Schematic of electrode-solution interphase (electric double layer). (Source: Kissinger and Heineman, 1996)

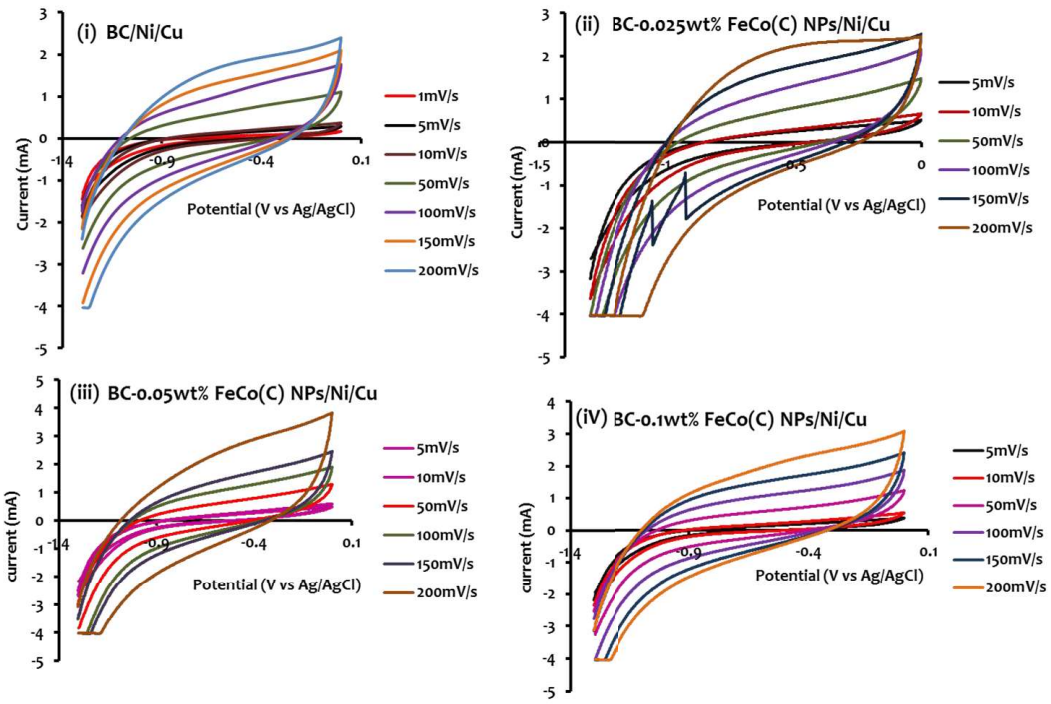

Figure 4.11 : Cyclic voltammogram of **(i)** black chrome and **(ii, iii & iV)** FeCo (C) NPs modified black chrome selective coatings with varying wt.% of FeCo(C) NPs deposited on nickel coated copper substrate, recorded with different scan rate (from 5 to 200 mVs-1), in 3.5 wt.% NaCl (saline) solution.

4.4.5.2 Linear Sweep Voltammetry: Corrosion

Tafel studies are carried out employing linear sweep voltammetry of black chrome and FeCo(C) NPs modified black chrome selective coatings deposited on copper and nickel coated copper substrates, as cathode, Pt coil as counter electrode and Ag/AgCl as reference electrode, in highly saline/marine environment of 3.5 wt.% NaCl electrolyte solution. The scan rate was varied from $1mVs^{-1}$ to $100mVs^{-1}$, to understand the corrosion impact on solar selective coatings in saline environments and effect of nanoparticles on the corrosion on black chrome coatings. The potentiodynamic polarization curve of BC and FeCo(C) NPs modified black chrome selective coatings on copper substrates are shown in Figure 4.12 left panel (i, ii, iii & iv), and used to calculate the numerous corrosion parameters. The corrosion potential (E_{corr}), corrosion current density (i_{corr}), corrosion resistance (R_P) and corrosion rate (C Rate) are summarized in respective tables of Figure .4.12 right panel (i, ii, iii & iv). The corrosion potential becomes more negative (-0.8467V to -1.1270V) with increasing the scan rate (from $1mVs^{-1}$ to $100mVs^{-1}$) for the pristine black chrome coatings (Fig.4.11, (left panel) Table (i)). The corrosion current density increases from 9.119 to 389.0 $\mu A/cm^2$, with increasing scan rate from $1mVs^{-1}$ to $100mVs^{-1}$. Similarly, corrosion rate has increased from 0.2598 to 11.08 mm/y, whereas corrosion resistance reduced from 7.805 to 0.0668 kΩ, with the scan rate from $1mVs^{-1}$ to $100mVs^{-1}$.

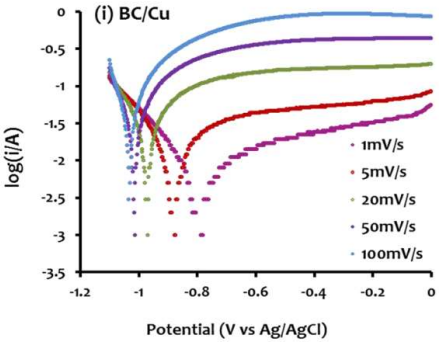

Tafel data					
	1mV/s	5mV/s	20mV/s	50mV/s	100mV/s
$E_{.corr}$ (V)	-0.8467	-0.9701	-1.0849	-1.1179	-1.1270
$I_{cor.}$ (A)	1.094E-5	3.23E-5	0.0001221	0.0002509	0.0004668
$i_{cor.}$ (μA/cm²)	9.119	26.94	101.8	209.1	389.0
R_p (KΩ)	7.805	2.437	0.5082	0.1619	0.06684
b_a (V/dec)	1.370	2.809	4.911	3.410	2.613
b_c (V/dec)	0.230	0.194	0.147	0.096	0.074
C. Rate (mm/y)	0.2598	0.7674	2.9	5.957	11.08

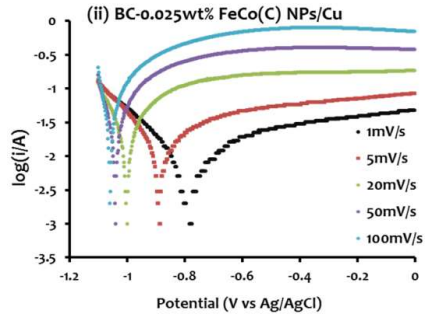

Tafel data					
	1mV/s	5mV/s	20mV/s	50mV/s	100mV/s
$E_{.corr}$ (V)	-0.8296	-0.8711	-0.9538	-1.0121	-1.0433
$I_{cor.}$ (A)	5.347E-5	7.023E-5	0.0001276	0.0002187	0.0003068
$i_{cor.}$ (μA/cm²)	44.56	58.62	106.3	182.2	255.7
R_p (KΩ)	1.611	1.139	0.5667	0.2993	0.204
b_a V/dec	1.184	0.982	1.160	1.415	1.537
b_c V/dec	0.238	0.227	0.194	0.169	0.159
C. Rate (mm/y)	1.269	1.667	3.028	5.191	7.287

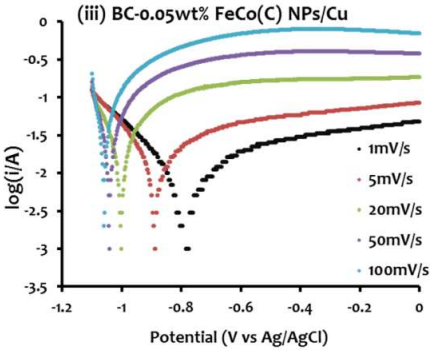

Tafel data					
	1mV/s	5mV/s	20mV/s	50mV/s	100mV/s
$E_{.corr}$ (V)	-0.8272	-0.9055	-1.0070	-1.0658	-1.0945
$I_{cor.}$ (A)	3.195E-5	5.686E-5	0.000147	0.0003018	0.0005264
$i_{cor.}$ (μA/cm²)	12.78	22.74	58.79	120.7	210.6
R_p (KΩ)	2.642	1.364	0.4549	0.1859	0.09297
b_a V/dec	1.050	1.237	1.747	2.037	2.123
b_c V/dec	0.239	0.209	0.169	0.138	0.119
C. Rate (mm/y)	1.222	2.175	5.623	11.55	20.14

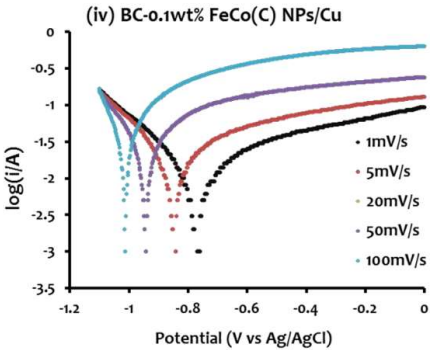

Tafel data					
	1mV/s	5mV/s	20mV/s	50mV/s	100mV/s
$E_{.corr}$ (V)	-0.8019	-0.8586	-0.9400	-1.0093	-1.0575
$I_{cor.}$ (A)	2.21E-5	3.636E-5	7.355E-5	0.000148	0.0002765
$i_{cor.}$ (μA/cm²)	8.842	14.54	29.42	123.3	230.4
R_p (KΩ)	3.553	2.028	0.9183	0.4038	0.1968
b_a V/dec	1.022	0.978	1.167	1.569	2.076
b_c V/dec	0.220	0.205	0.179	0.151	0.133
C. Rate (mm/y)	0.8457	1.391	2.814	3.514	6.564

Figure 4.12 : (Left Panel) Potentiodynamic polarization curve of **(i)** black chrome and **(ii, iii&iv)** FeCo(C) NPs modified black chrome solar selective coatings with varying wt.% of FeCo(C) NPs deposited on copper substrates, in 3.5wt.% (Saline) NaCl solution, with varying scan rate (1mVs^{-1} to 100 mVs^{-1}). **(Right Panel) (Table i, ii, iii&iv)** represents the estimated corrosion parameter of black chrome and FeCo(C) NPs modified black chrome selective coatings with varying wt.% of FeCo(C) NPs on copper substrates through Tafel fitting of polarization curves.

The potentiodynamic curves are shown in Figure 4.12(ii) for 0.025wt.% FeCo(C) NPs modified black chrome selective coating and respective corrosion parameters are summarized in Table (ii). Corrosion resistance value is relatively lower for 0.025wt.% modified black chrome selective coatings as compared to pristine black chrome at low scan rate (1 - 5 mVs^{-1}), while at higher scan rate (20 mVs^{-1} - 100 mVs^{-1}) the corrosion resistance values became larger (0.5667 kΩ to 0.204 kΩ) as compared to that of pristine black chrome selective coatings (0.5082 to 0.06684 kΩ). These measurements suggest that 0.025wt.% FeCo(C) NPs modified black chrome coatings exhibit enhanced corrosion resistance as compared to that of pristine black chrome structures. The similar behavior has been observed for 0.05wt.% and 0.10wt.% FeCo(C) NPs modified black chrome spectrally selective coatings on Cu substrates, as shown in Figure 4.13, where corrosion resistance has been plotted against the scan rates. These results suggest that corrosion rate has reduced to half (6.564 mm/y) for 0.1 wt.% FeCo(C) NPs modified black chrome selective coatings, as compared to the pristine black chrome (11.08 mm/y) at 100 mVs^{-1} scan rate.

The observed enhancement in corrosion resistance for FeCo(C) NPs modified black chrome structures is consistent with the measured lower corrosion rate for FeCo(C) NPs modified black chrome. This also suggests that FeCo(C) NPs may be providing a protective coating on chromium metallic structures in black chrome coatings and thus avoiding direct access to the corrosive media. These observations corroborate the proposed hypothesis, as shown in Figure 4.1. This enhancement in corrosion resistance may be due to the environmentally stable graphite encapsulated FeCo(C) NPs and their effective distribution in the cermet matrix. Corrosion study on black chrome and FeCo(C) NPs modified black chrome selective coatings on nickel coated copper substrates also showed similar behavior as on copper substrate and details are summarized in Usmani et al. reference [Usmani and Harinipriya, 2013].

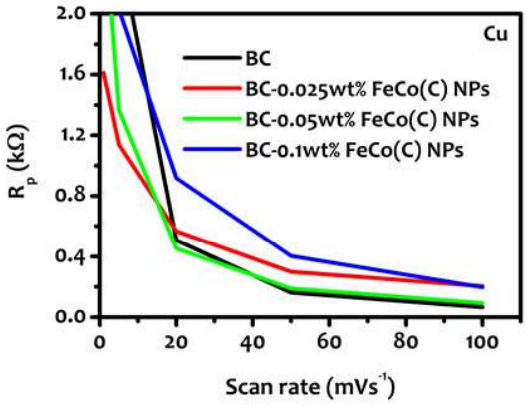

Figure 4.13 : Corrosion resistance vs. scan rate of black chrome and FeCo(C) NPs modified black chrome with varying wt.% of NPs selective coatings on copper substrates.

4.4.6 Thermal Stability

Thermal stability tests for these coating structures are carried out using thermogravimetric analysis, in inert environmental conditions. The measurements are summarized in Figure 4.14, in the form of percent weight change as a function of temperature for black chrome and FeCo(C) NPs modified black chrome selective coatings, deposited on copper and nickel coated copper substrates, respectively. Pristine black chrome coatings on copper substrate showed an initial weight change ~ 0.85% up to 350°C, and remained nearly

constant up to 700°C, in N_2 environment, as can be seen in Figure 4.14 (left panel). The initial percentage weight change is attributed to the loss of volatile components such as unburnt organics during the synthesis and post synthesis processes. However, the weight gain observed after 700°C is attributed to the formation of higher molecular weight compounds such as chromium nitride (CrN), nitrous oxides (N_2O), or even Cr_2O_3 due to the oxidation of metallic chromium in black chrome matrix. The instability of nitrogen molecule at a higher temperature, may be responsible for the formation of nitride compounds in nitrogen environmental conditions and residual oxygen may lead to the oxidation of metallic chromium. FeCo(C) NPs modified black chrome selective coatings on copper substrate showed enhanced thermal stability as compared to the pristine one, as can be seen in Figure 4.14 (left panel). A relatively lower weight change ~ 0.31% has been observed initially, from 120 °C to 220 °C with FeCo(C) NPs modified black chrome selective coatings, and is attributed to the loss of volatile components, as also observed in pristine BC structure. The coating is further relatively stable up to 730°C. Here also the observed weight gain after 730 °C, is due to the formation of degradation products of higher molecular weight, as in the case of pristine black chrome coatings. Higher thermal stability of FeCo(C) NPs modified black chrome selective coatings is attributed to the protective coating of thermally stable FeCo(C) NPs on metallic chromium in black chrome matrix. These results indicate that 0.05wt.% FeCo(C) NPs modified black chrome selective coatings is relatively better thermally stable as compared to 0.025 and 0.1wt.% of nanoparticles modified black chrome selective coatings.

Figure 4.14 (right panel), shows the percentage weight change of black chrome and FeCo(C) NPs modified black chrome selective coatings on nickel coated copper substrates, as a function of temperature. These measurements also suggest that the thermal stability of FeCo(C) NPs modified black chrome selective coatings on nickel coated copper substrates is better as compared to that of black chrome structures only. More surprisingly, spectrally selective structures on Ni/Cu show enhanced thermal stability as compared to that of bare Cu substrate. The relative thermal stability of Ni in Ni/Cu provides better thermally stable spectrally selective structures as compared to that of on Cu substrates only. Pristine black chrome coatings on nickel coated copper substrate showed an initial weight loss like coatings on an uncoated copper substrate. The observed initial percentage weight change is attributed to the loss of volatile components such as unburnt organics, as observed and discussed previously for coatings on Cu substrates. Here also, the observed weight gain after 800°C is attributed to the formation of higher molecular weight compounds such as chromium nitride (CrN), nitrous oxides (N_2O), or even Cr_2O_3 due to the instability of nitrogen molecule at higher temperature and oxidation of metallic chromium in black chrome matrix. Moreover, graphite encapsulated FeCo modified black chrome selective films showed relatively better thermal stability, Figure 4.14 (right panel), similar to that of uncoated nickel copper substrate.

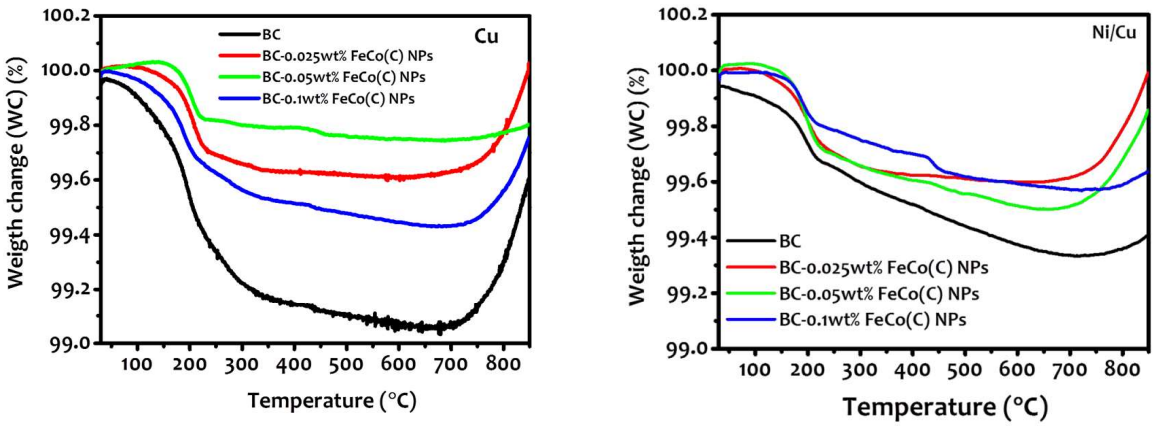

Figure 4.14 : Percentage weight change as a function of temperature for black chrome and FeCo(C) NPs modified black chrome selective coatings with varying wt.% of NPs deposited on **(left)** copper and **(right)** nickel coated copper substrate, in an inert atmosphere.

4.5 ANALYSIS AFTER ELECTROCHEMICAL MEASUREMENTS

The structural, microstructural and compositional analysis of this corrosion treated black chrome and FeCo(C) NPs modified black chrome spectrally selective coatings have been investigated in detail to understand the possible degradation and structure-property correlation, as discussed below.

4.5.1 Structural, Microstructural, and Elemental Analysis after Electrochemical Measurements

X-ray diffraction spectra of cyclic voltammetry treated black chrome and FeCo(C) NPs modified black chrome selective coatings on copper substrates, are shown in Fig. 4.15 a(i, ii, iii & iv) (left panel). These XRD measurements suggest that there are no structural changes in case of FeCo(C) NPs modified black chrome coatings and diffraction spectra are nearly identical to that of the pristine ones, as shown and discussed in section 4.4.1. The pristine black chrome structures exhibited additional diffraction peaks at 2θ = 44.34° (110) and 64.80° (200), which correspond to the cubic chromium phase (ICDD #: 01-077-7591) (Fig.4.15 a(i)), after corrosion treatments. The onset of additional chromium diffraction peaks in pristine black chrome suggests that the corrosion has initiated and degraded black chrome layer, whereas corrosion, has the least impact on FeCo(C) NPs modified black chrome coating structures.

Figure 4.15 b(i, ii, iii & iv), shows the X-ray diffraction spectra of black chrome and FeCo(C) NPs modified black chrome selective coatings deposited on copper substrates, after corrosion measurements. The similar XRD patterns have been recorded after the corrosion measurements for FeCo(C) NPs modified black chrome structures, suggesting relative inertness to the corrosion as compared to pristine black chrome, where additional chromium diffraction peaks have been recorded, as shown in Figure 4.15 b(i). Structural properties exhibit similar crystallographic phases for black chrome and FeCo(C) NPs modified black chrome selective coatings on nickel coated copper and SS substrates as on copper substrates.

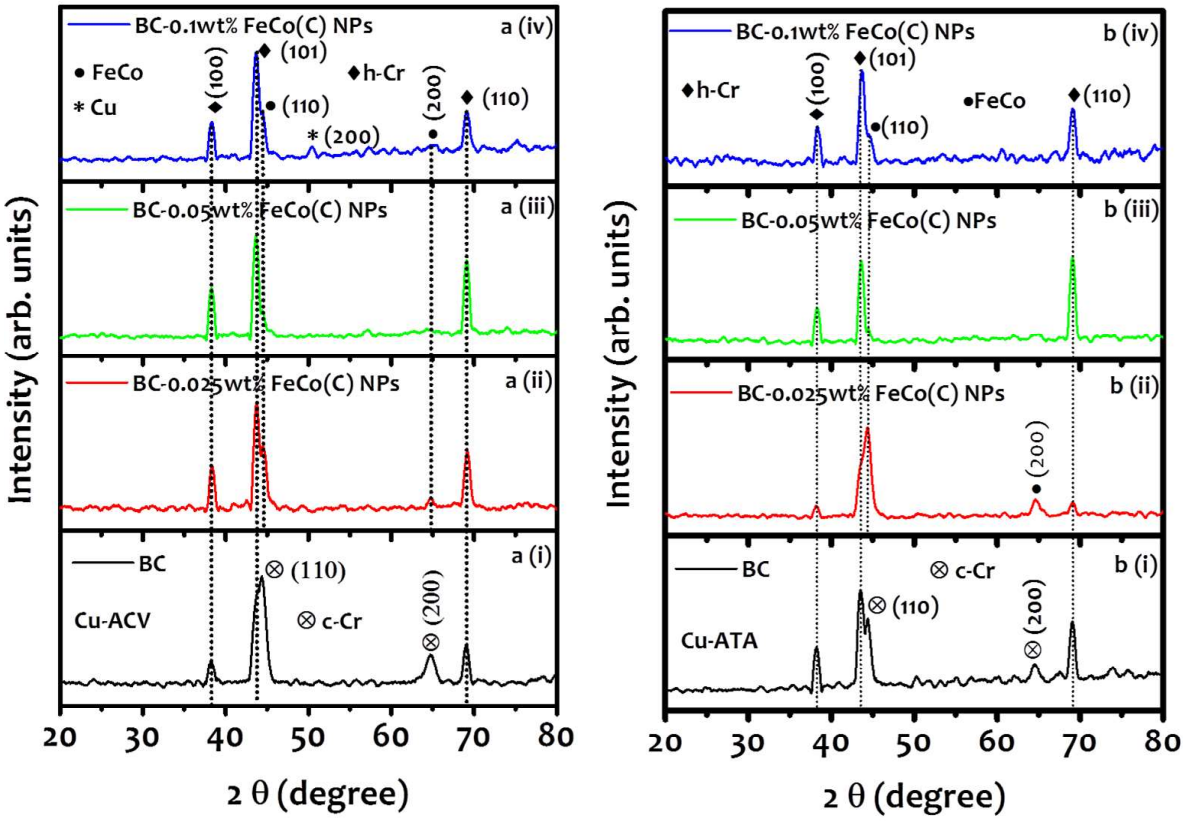

Figure 4.15 : X-ray diffraction spectra of (a&b)(i) black chrome and (a&b)(ii, iii, iv) FeCo(C) NPs modified black chrome selective coatings with varying wt.% of FeCo(C) NPs deposited on copper substrates, (left panel) after Cyclic voltammetry measurements and (right panel) after corrosion measurements.

Figure 4.16 shows the SEM surface microstructure of black chrome (Fig.4.16 (a)(i)) and FeCo(C) NPs modified black chrome selective coatings on copper substrate (Fig.4.16 a(ii, iii & iv)), after cyclic voltammetry measurements. These measurements suggest that the grain size of pristine black chrome coating has changed from micro to needle-shaped nano grains after cyclic voltammetry measurements (Fig.4.16 (a)(i)). Moreover, cracks on pristine black chrome selective coatings are completely filled and became much denser, after cyclic voltammetry measurements. 0.025wt.% FeCo(C) NPs modified black chrome selective coatings surface microstructure, Fig.4.16 a(ii), becomes much smoother and the cracks were partially filled with composite particles after cyclic voltammetry measurements. Surface microstructure of 0.05wt.% FeCo(C) NPs modified black chrome selective coatings, Fig. 4.16 a(iii), is showing the hybrid nature containing partially smooth and partially denser nano grains. The cracks were filled with denser nanoparticles, whereas the already existing islands at smooth regions of the coatings also co-existed (Fig.4.3 (c)). Fig.4.16 a(iv), shows the surface microstructure of 0.1wt.% FeCo(C) NPs modified black chrome selective coatings, after cyclic voltammetry measurements. The cracks are filled and the grains have changed drastically from micro to needle-shaped nano grains. This anomalous behavior may be attributed to the variation in the diffusion of ions and mass transfer rates of the active species in the spectrally selective structures.

Figure 4.16 b(i) shows the surface microstructure of pristine black chrome selective coatings on a copper substrate, after corrosion measurements. This SEM study reveals that the particle size changed drastically from micron size grains to nano sized grains and the geometry of the surface becomes more needle like, indicating the corrosion impact on these surfaces. However, the surface microstructure of 0.025wt.% modified black chrome selective coatings

(Fig. 4.16 b(ii)), suggests that cracks on the surface are almost covered, with enhanced surface roughness. 0.05wt.% FeCo(C) NPs modified black chrome selective coatings surface microstructure, Fig. 4.16 b(iii), suggests the entire coverage of cracks and boils, due to the corrosion effects on the surface. Surface microstructure of 0.1wt.% FeCo(C) NPs modified black chrome selective coatings, Fig.4.16 b(iv), do not show any effect on the surface microstructure, suggesting that corrosion has the least impact on this structure. From the above SEM microstructural analysis, it is evident that the stability of FeCo(C) NPs modified black chrome coatings has enhanced even in saline environments. The similar analysis of these coatings on Ni/Cu substrates are discussed in detail by Usmani et al. [Usmani and Harinipriya, 2013].

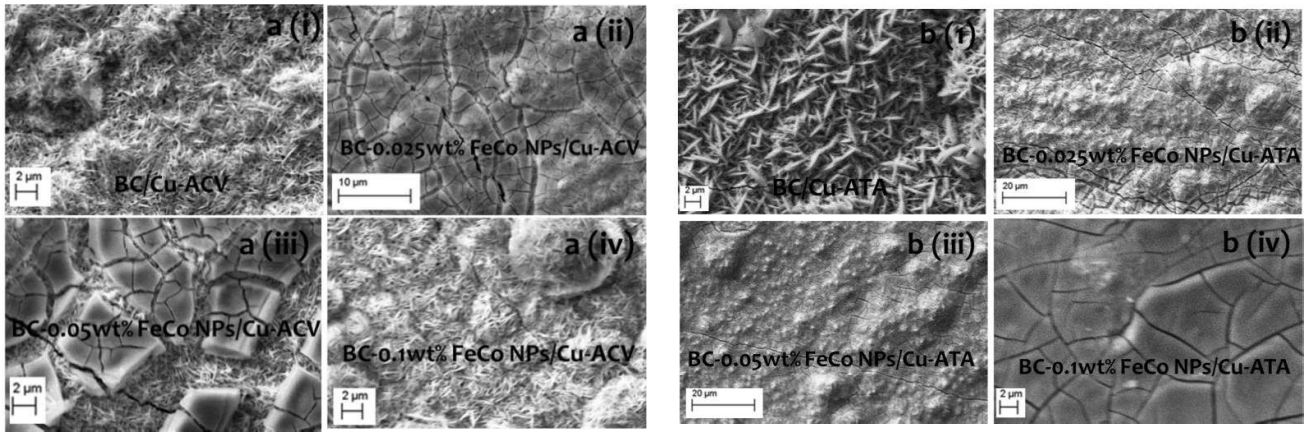

Figure 4.16 : SEM surface micrographs of (a & b)(i) black chrome and (a & b)(ii, iii, iv) FeCo(C) NPs modified black chrome selective coatings with varying wt.% of FeCo(C) NPs deposited on copper substrates, (left panel) after Cyclic voltammetry measurements and (right panel) after corrosion measurements.

After cyclic voltammetry measurements, atomic force microscopy (AFM) measurements are shown in Figure 4.17 a(i, ii, iii & iv) (left panel) for black chrome and FeCo(C) NPs modified black chrome selective coatings on the copper substrate. These measurements also confirmed the similar surface microstructural features, as observed in SEM micrographs. Average surface roughness has increased for 0.025 and 0.05 wt.% FeCo(C) NPs modified black chrome selective coatings, as shown graphically in Fig. 4.17 (right panel). This is due to the partially filled cracks and a mixture of partially smooth and partially denser nano grains regions, as also has been observed in SEM surface microstructure analysis, Fig. 4.16 a(ii & iii) (left panel).

AFM surface morphology of black chrome and FeCo(C) NPs modified black chrome selective coatings on a copper substrate after corrosion measurements are shown in Figure 4.18 b(i, ii, iii & iv). The average surface roughness (R_a) of these coatings has decreased with increasing wt.% of FeCo(C) NPs in modified black chrome selective coatings (Fig. 4.18(right panel)), which is mainly attributed to the reduction in cracks and other surface irregularities as shown in Figure 4.16 b(ii, iii & iv), also substantiating the SEM findings, as discussed previously.

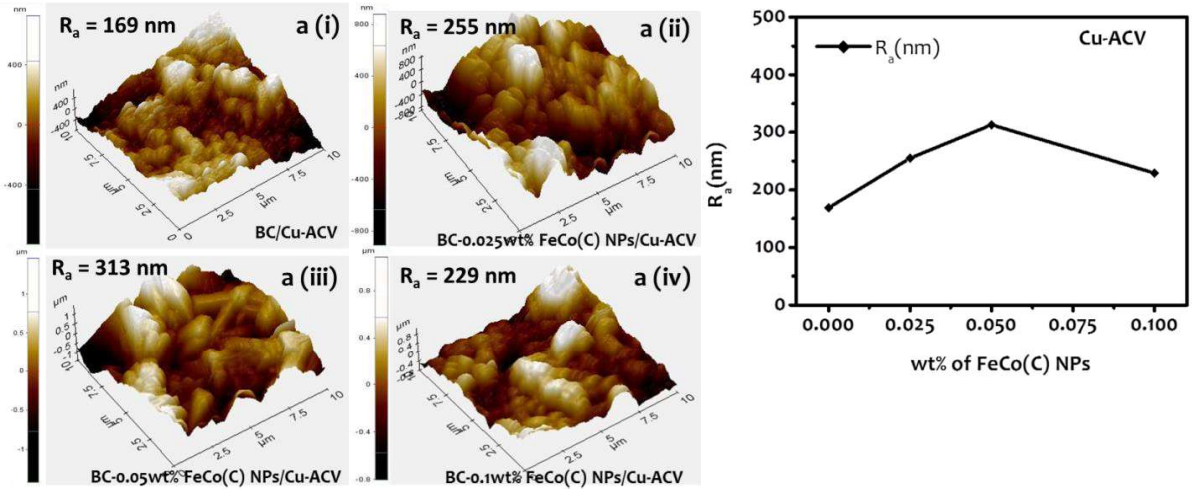

Figure 4.17 : (left panel) AFM surface morphology of (a)(i) black chrome and (a)(ii, iii, iv) FeCo(C) NPs modified black chrome selective coatings with varying wt.% of FeCo(C) NPs deposited on copper substrates, after Cyclic voltammetry measurements and **(right panel)** average surface roughness (R_a) with varying wt.% of FeCo(C) NPs.

Energy Dispersive X-ray (EDS) spectra of black chrome and FeCo(C) NPs modified black chrome selective coating on copper substrate are shown in Figure 4.19 a(i, ii, iii & iv) after cyclic voltammetry (CV) measurements, and in Figure 4.20 b(i, ii, iii & iv) after corrosion measurements. The corresponding elemental composition in weight% and atomic% are represented as insets in these EDX spectra (Fig.4.19 a(i, ii, iii & iv) & Fig. 20 b(i, ii, iii & iv)). After cyclic voltammetric measurements, oxygen and chromium atomic fractions are 36.11 atm.% and 63.89 atm.%, (Fig.4.19 a(i)), respectively. These atomic fractions have changed drastically as compared to 74.58 atm.% and 25.42 atm.% fractions of oxygen and chromium before CV measurements (Fig.4.6 (a)). The similar changes have been observed for FeCo(C) NPs modified black chrome coatings after cyclic voltammetry measurements, where, as an example, oxygen atomic fraction has reduced from 64.22 atm.% (before cyclic voltammetry measurements) to 51.50 atm.% and chromium atomic fraction has increased from 27.63 atm.% (before cyclic voltammetry measurements) to 42.80 atm.% for 0.025 wt.% FeCo(C) NPs modified black chrome coatings. The changes in the atomic fraction of elemental compositions have been summarized in respective Tables. In addition to the observed expected elements, some undesired elements have also been observed such as sodium, chlorine in very small atomic fractions in the case of cyclic voltammetry treated coating structures. The presence of these undesired elements may be due to the saline electrolyte solution used for these cyclic voltammetry experiments.

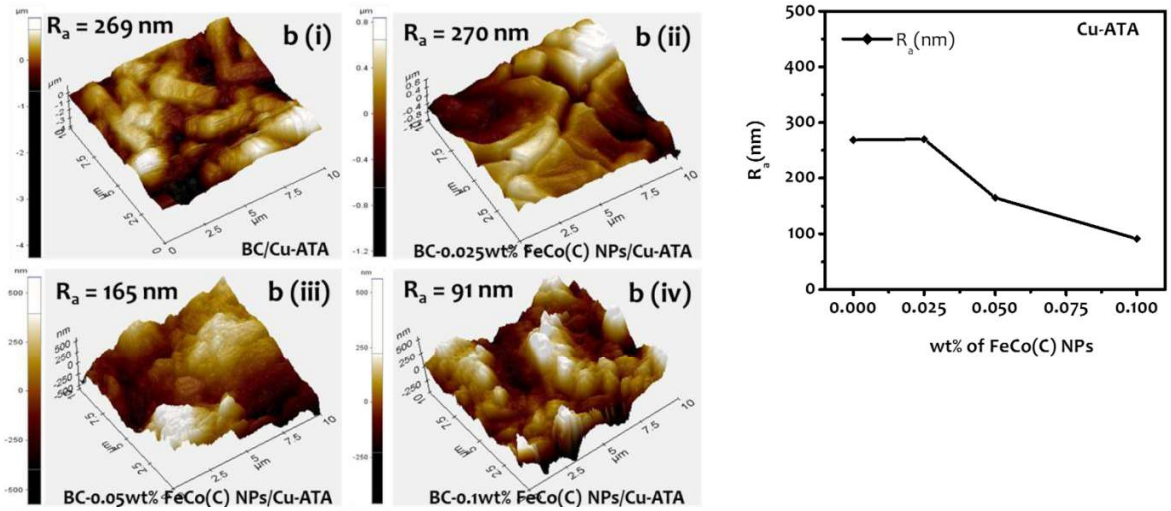

Figure 4.18 : (left panel) AFM surface morphology of (b)(i) black chrome and (b)(ii, iii, iv) FeCo(C) NPs modified black chrome selective coatings with varying wt.% of FeCo(C) NPs deposited on copper substrates, after corrosion measurements and **(right panel)** average surface roughness (R_a) with varying wt.% of FeCo(C) NPs.

The similar trends for an atomic fraction of different elements have also been observed after corrosion measurements for black chrome and FeCo(C) NPs modified black chrome selective coatings, Figure 4.20 b(i, ii, iii & iv). The elemental analysis has been carried out at different regions and observed that FeCo(C) NPs are distributed homogeneously and avoiding the oxidation of metallic chromium in FeCo(C) NPs modified black chrome coatings. Thus, the environmental stability of the black chrome has increased relatively after the modification of graphite encapsulated FeCo nanoparticles (FeCo(C) NPs). The similar observations have been observed in the case of FeCo(C) NPs modified black chrome selective coatings on nickel seeded copper substrate, after cyclic voltammetry and corrosion measurements and discussed by Usmani et al. in detail [Usmani and Harinipriya, 2013].

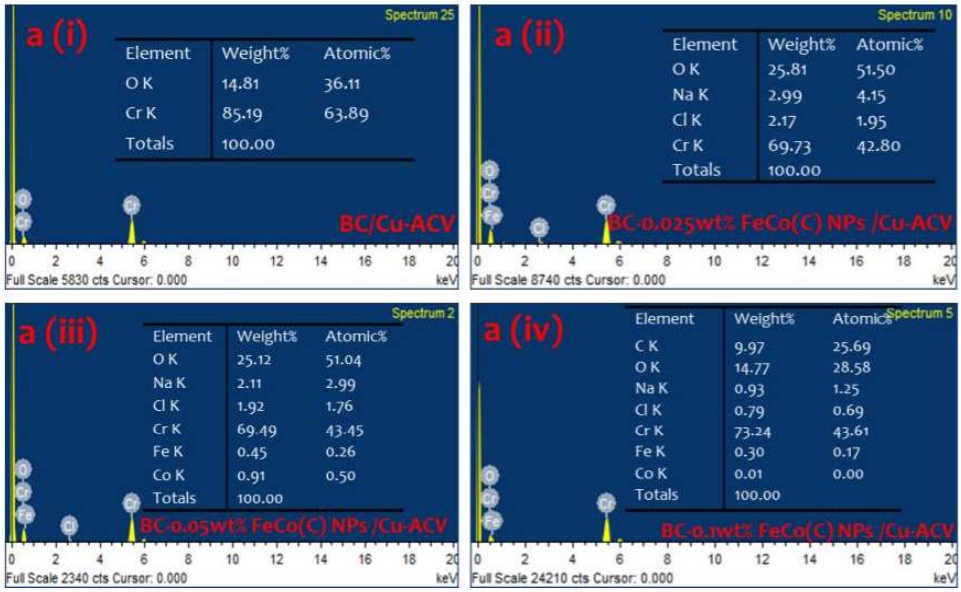

Figure 4.19 : EDS elemental analysis of (a)(i) black chrome and (a)(ii, iii, iv) FeCo(C) NPs modified black chrome selective coatings with varying wt.% of FeCo(C) NPs deposited on copper substrates, after cyclic voltammetry measurements.

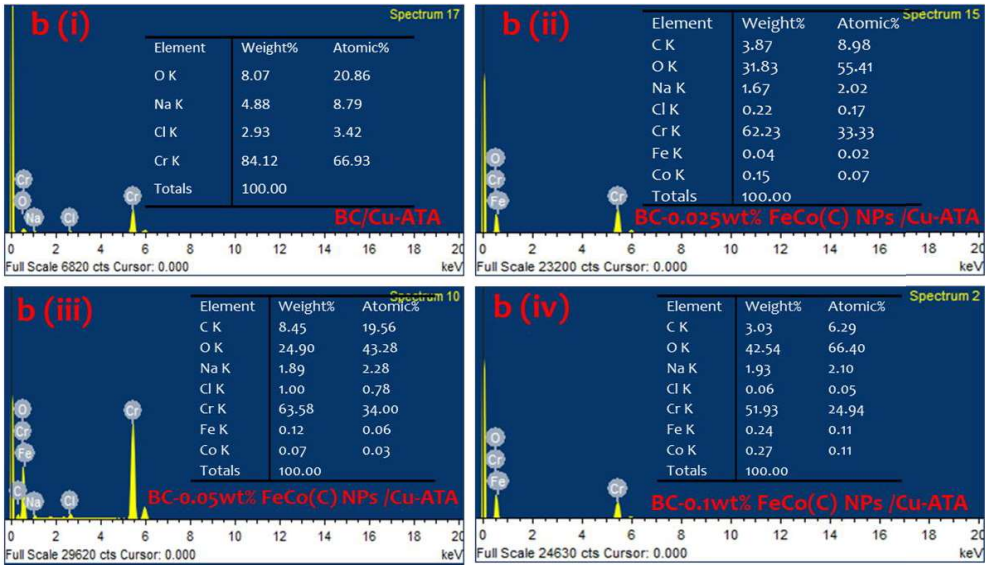

Figure 4.20 : EDS elemental analysis of (b)(i) black chrome and (b)(ii, iii, iv) FeCo(C) NPs modified black chrome selective coatings with varying wt.% of FeCo(C) NPs deposited on copper substrates, after corrosion measurements.

4.5.2 Optical Properties after Electrochemical Measurements

The measured reflectance spectra in 200 – 800 nm wavelength range of black chrome and FeCo(C) NPs modified black chrome selective coatings on Cu and Ni/Cu substrates, are shown in Figure 4.21 (a & b). These measurements were recorded after cyclic voltammetric measurements on these coating structures and used for calculating absorptance for these structures. The calculated absorptance values are summarized in the respective insets of Figure 4.21 (a & b). The absorptance values are ~ 0.96 for all these structures after CV measurements, especially on Cu substrates, whereas absorptance values are ~ 0.95, on Ni/Cu substrates. The observed changes are really insignificant and are within the error limits of measurements and related calculations.

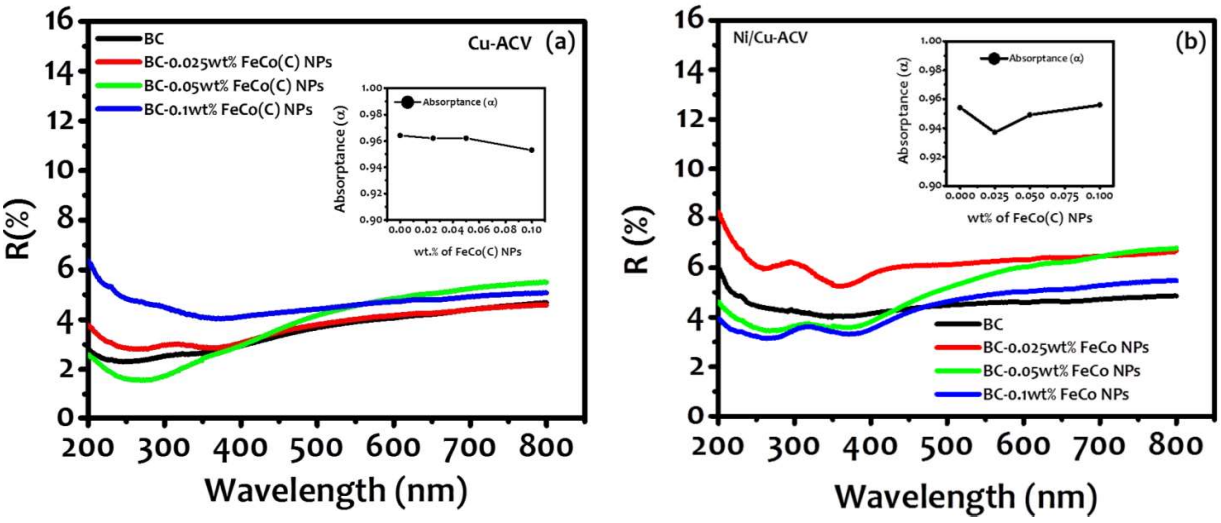

Figure 4.21 : reflectance spectra versus wavelength of black chrome and FeCo(C) NPs modified black chrome selective coatings with varying wt.% of FeCo(C) NPs deposited on **(a)** Cu and **(b)** nickel coated Cu substrates, after cyclic voltammetry measurements. Calculated absorptance values vs. varying wt.% of FeCo(C) NPs have represented an inset in the graphs a & b.

Figure 4.22 (a & b) summarizes reflectance spectra of BC and FeCo(C) NPs modified BC selective coatings in 2.5 – 25 μm wavelength range, after CV measurements, and used to calculate the emittance values. The measured emittance values are shown as insets in Figure 4.22 (a & b). These values are relatively on the higher side and are nearly similar to the values for coatings without cyclic voltammetry and corrosion measurements. However, FeCo(C) NPs modified black chrome selective coatings on both copper and nickel coated copper substrate showed relatively lesser emittance values, after CV measurements. These observations suggest that FeCo(C) NPs modified black chrome selective coatings may be more environmentally stable as compared to the pristine black chrome coatings and thus can be used under saline conditions, and at elevated temperatures.

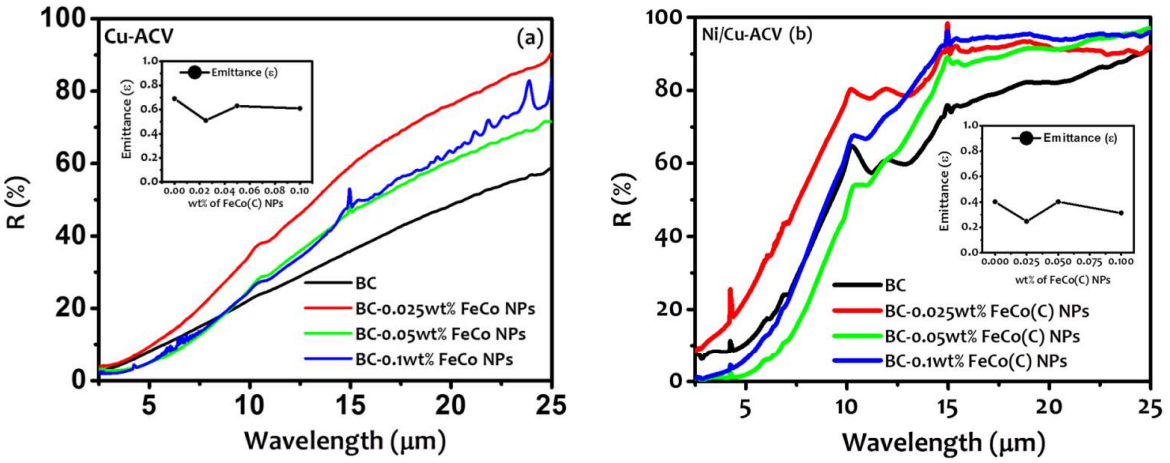

Figure 4.22: reflectance spectra verses wavelength in the range of 2.5 – 25 μm of black chrome and FeCo(C) NPs modified black chrome with varying wt.% of FeCo(C) NPs selective coatings deposited on (a) copper (b) nickel coated Copper substrates, after cyclic voltammetry measurements. Calculated emittance values vs. varying wt.% of FeCo(C) NPs have represented an inset in the graphs.

4.6 CONCLUDING REMARKS

These studies suggest that only hexagonal chromium (Cr) phase in pristine black chrome selective coatings. However, FeCo(C) NPs modified black chrome selective coatings exhibit a hexagonal chromium phase in conjunction with the cubic iron cobalt (FeCo) phase, substantiating the introduction of FeCo(C) nanoparticles in black chrome matrix. Moreover, chromium oxide (Cr_2O_3) phase has not been observed in X-ray diffraction and is mainly due to its amorphous nature in the coating matrix. Pristine black chrome exhibited relatively smoother surface with large surface cracks. Elemental analysis has confirmed that FeCo(C) NPs are evenly distributed in the black chrome selective coatings. FeCo(C) NPs modified black chrome selective coatings also do not exhibit any significant any changes in absorptance values (> 0.94), as compared to the pristine black chrome coatings. However, the emittance values for these coatings are quite high (0.47) because of the relatively larger thickness of these coatings. Electrochemical measurements revealed that the FeCo(C) NPs modified black chrome selective coatings may provide enhanced corrosion resistance and environmental stability as compared to the pristine black chrome selective coatings. Thermal stability analysis confirms that FeCo(C) NPs modified black chrome selective coatings are more thermally stable as compared to the pristine ones. Thus, FeCo(C) NPs modified black chrome spectrally selective coatings can be used in open ambient due to their high corrosion resistance and also at relatively higher temperature applications such as in concentrated solar power applications, which may not be possible for pristine black chrome coatings.

…